

Synthesis, pharmacokinetics, and biological use of lysine-modified single-walled carbon nanotubes

J Justin Mulvey^{1,2}
Evan N Feinberg^{1,3}
Simone Alidori¹
Michael R McDevitt^{4,5}
Daniel A Heller^{1,6}
David A Scheinberg^{1,5,6}

¹Molecular Pharmacology and Chemistry Program, Sloan Kettering Institute, New York, NY, USA;

²Tri-Institutional MD-PhD Program, New York, NY, USA; ³Department of Applied Physics, Yale University, New Haven, CT USA; ⁴Department of Radiology and ⁵Department of Medicine, Memorial Sloan Kettering Cancer Center, New York, NY, USA;

⁶Weill Cornell Medical College, New York, NY, USA

Abstract: We aimed to create a more robust and more accessible standard for amine-modifying single-walled carbon nanotubes (SWCNTs). A 1,3-cycloaddition was developed using an azomethine ylide, generated by reacting paraformaldehyde and a side-chain-Boc (tert-Butyloxycarbonyl)-protected, lysine-derived alpha-amino acid, H-Lys(Boc)-OH, with purified SWCNT or C60. This cycloaddition and its lysine adduct provides the benefits of dense, covalent modification, ease of purification, commercial availability of reagents, and pH-dependent solubility of the product. Subsequently, SWCNTs functionalized with lysine amine handles were covalently conjugated to a radiometalated chelator, 1,4,7,10-tetraazacyclododecane-1,4,7,10-tetraacetic acid (DOTA). The ¹¹¹In-labeled construct showed rapid renal clearance in a murine model and a favorable biodistribution, permitting utility in biomedical applications. Functionalized SWCNTs strongly wrapped small interfering RNA (siRNA). In the first disclosed deployment of thermophoresis with carbon nanotubes, the lysine-modified tubes showed a desirable, weak SWCNT-albumin binding constant. Thus, lysine-modified nanotubes are a favorable candidate for medicinal work.

Keywords: fullerene, cycloaddition, azomethine, DOTA, thermophoresis, ¹¹¹In

Introduction

The chemical and physical structure of single-walled carbon nanotubes (SWCNTs) confers unique spatial, mechanical, pharmacokinetic, and electronic properties.^{1,2} Methods exist to conjugate SWCNTs to a variety of moieties, with the goal of modifying or exploiting these properties in fields such as circuitry, imaging,³ and drug delivery. For instance, the extensive π -system of carbon nanotubes allows noncovalent nucleotide wrapping and the adherence of other π -stacking molecules, such as aromatic pharmaceuticals.⁴⁻⁶ Covalent modifications act as chemical handles for the attachment of radiometals,^{7,8} adjuvants, oligonucleotides,⁹ fluorophores,¹⁰ targeting agents,¹¹⁻¹³ and receptor ligands. Covalent approaches include radical-driven additions,^{14,15} the Bingel-Hirsch cyclopropanation reaction,^{16,17} and azomethine ylide-driven 1,3-cycloadditions,¹⁸⁻²⁰ among others, such as carboxylation and Grignard reactions.²¹⁻²³ The regiochemistry of the applicable reactions favors addition across [6, 6] over [6, 5] carbon-carbon bonds found on SWCNT caps and spherical fullerenes; calculations have shown that adducts to the [6, 6] carbons are more thermodynamically stable, driven in part by the bond's more conducive π -orbital and alkene-like character.^{24,25} Identical reaction mechanisms and products on C60 buckminsterfullerene (or "buckyballs"), a discrete and homogeneous allotrope of carbon, served as a platform in this work, to aid in the structural elucidation of SWCNT adducts that are resistant to standard spectroscopy methods.

Solubilization of SWCNTs and spheroid fullerenes through these covalent modifications confers the added advantage of dispersing aggregates and reducing

Correspondence: David A Scheinberg
Sloan Kettering Institute, 1275 York
Avenue, New York,
New York 10065, USA
Fax +1 646 888 2195
Email d-scheinberg@ski.mskcc.org

toxicity and immunogenicity, which increases their potential as pharmacologic agents.^{26–32} Commonly employed among 1,3-cycloadditions is the Prato reaction³³ – an adaptation of chemistry developed by Tsuge and Kanemasa¹⁸ – which solubilizes and aminates fullerenes with a Boc (tert-Butyloxycarbonyl)-protected, pegylated pyrrolidine bearing both a primary and a tertiary amine (1) (Figure 1A).

The method herein described begets an amine handle with similar functionality yet distinct properties that bears a secondary amine, rather than a tertiary amine, in addition to the primary amine (Figure 1B). The product, SWCNT-lysine (Lys)-NH₂ (2) is more soluble in acidic and pH neutral polar-protic solvents, despite its lack of an ethoxy sidearm, but is less soluble than (1) in basic solutions; this property allows for convenient, solubility-based purifications. As with (1), it has been demonstrated that (2) accepts covalently attached structures via its primary amine. The solubility conferred by this functionalization enables (2) to rapidly clear via the kidney, akin to previous murine excretion study findings on (1).²⁷ Relative to the standard method that produces (1), this reaction generates 40% more amine handles per SWCNT carbon, is more stable to degradation, and uses

a comparatively inexpensive starting material: an easily obtained amino acid.

The utility of (2) and its suitability for biomedical applications were explored in the present study, including small interfering RNA (siRNA)-carrying capacity, biodistribution, and pharmacokinetics in mice, as well as the first use of thermophoresis to measure nanotube–protein binding.

Materials and methods

Covalent functionalization of SWCNTs and C60

Pristine SWCNTs produced by the chemical vapor deposition (CVD) CoMoCAT[®] method (SWeNT[®] CG-100; Sigma-Aldrich Corp, St Louis, MO, USA) were sonicated for 30 minutes in a pH 8 ethylenediaminetetraacetic acid (EDTA) solution. The SWCNTs were then washed with metal-free water and in 7N HNO₃ at reflux for 5 minutes, to remove carbonaceous impurities and residual metals. The resultant SWCNTs were filtered over fritted glass and washed with metal-free water to normalize the pH. The tubes were then dried and reacted, in a 500 mL round-bottom flask, with the alpha amino-acid lysine bearing a Boc-protected side chain (H-Lys(Boc)-OH; Chemical Abstracts Service [CAS] registry number 2418-95-3) (Santa Cruz Biotechnology, Dallas, TX, USA), as well as paraformaldehyde in N,N-dimethylformamide (both from Sigma-Aldrich Corp, St Louis, MO, USA), in a 1:2:2 molar ratio (SWCNT:PFA:Amino Acid) based on the moles of SWCNT carbon by weight. This was a fourfold excess of nonnanotube reagents, as each ylide bridges two carbon atoms. This mixture was heated to 130°C for 5 days with H-Lys(Boc)-OH and paraformaldehyde added in amounts of 20% allotments of their total stoichiometric mass per day. An equivalent procedure was used in the production of (1), with the substitution of (2,2-dimethyl-4-oxo-3,8,11-trioxa-5-azatridecan-13-yl)glycine (Discovery ChemScience LLC, Princeton, NJ, USA).

Upon completion, the opaque, black mother liquor was filtered over a glass frit, followed by filtration through a Millipore polytetrafluoroethylene (PTFE) filter (0.2 μm pore size) with metal-free water to remove unreacted solids, resulting in a translucent amber-brown filtrate that was dried, by rotary evaporation, to a dark-brown oil.

The resulting oil was dialyzed with a 3,500 molecular weight cutoff (MWCO) Slide-A-Lyzer[®] cassette (Thermo Fisher Scientific Inc., Waltham, MA, USA). The retentate was collected and acidified with HCl to pH 4, then washed with ethyl acetate. The aqueous fraction was then recollected and washed with CHCl₃. The aqueous fraction was

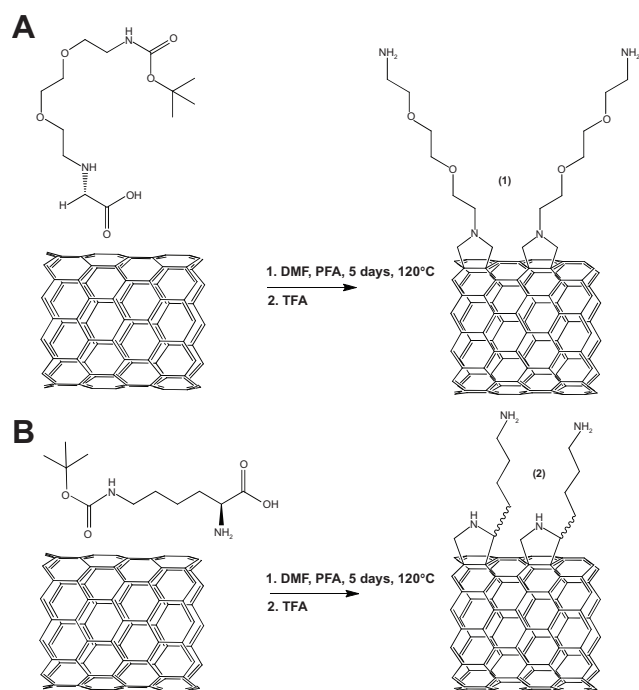


Figure 1 (A) 1,3-cycloaddition of Prato reaction with synthesized amine-modified glycine (B) 1,3-cycloaddition employing purchasable H-Lys(Boc)-OH, with handle emerging from the chiral carbon center.

Abbreviations: DMF, dimethylformamide; PFA, paraformaldehyde; TFA, trifluoroacetic acid; Boc, (tert-Butyloxycarbonyl); Lys, lysine.

collected, and basified with NaOH at 50°C until it became cloudy and then was allowed to cool, forming a layer of brown powder. This biphasic solution was then filtered, and the precipitate was lightly washed with ice water. The solid was collected in pH 7 metal-free water, frozen, and dried by lyophilization. If the unprotected construct was desired, the Boc groups were removed by stirring the product in neat trifluoroacetic acid for 2 hours at 50°C before quenching with metal-free water, dialyzing, and rotovapping or lyophilizing, to obtain (2). Conditions were kept metal-free, with future radiolabeling in mind, but these conditions are not necessary.

The reaction with C60 was performed identically, except the wash with 7N HNO₃ was completed at room temperature (RT) for only 5 minutes, to limit fragmentation of the more reactive buckyballs, and the reaction progressed in dimethylformamide at 100°C, with reagents added over 3 days instead of 5, giving (3).

Boc-protecting group presence or removal was confirmed by nuclear magnetic resonance (NMR) and infrared (IR) spectroscopy, and a Kaiser/Sarin assay, before and after removal, was used as a measure of amine content. Yield of the final product, SWCNT-Lys-NH₂ (2), compared with the acid-washed starting SWCNTs was 30%. Unreacted material could be re-reacted twice more, for a combined yield of 58%. Reducing the reaction time from 5 to 4 days had no effect on yield. Yield of the modified C60 ranged from 85%–96%. Removing Boc before the described pH- and solubility-based separations resulted in lower yield. Degradation of (1) and (2) was monitored through NMR comparisons at ~30 days after the initial NMR was taken. Samples were kept in their original tubes at RT. Light exposure had minimal discrepancies.

Mass spectroscopy was conducted on a Waters SQ Detector (Waters Corporation, Milford, MA, USA) with MassLynx and Spectrum software (Waters Corporation). Ultraviolet-visible spectrophotometry (UV-Vis) analysis was conducted on a SpectraMax® M2 Multi-Mode Microplate Reader from Molecular Devices (Sunnyvale, CA, USA). High-performance liquid chromatography (HPLC) analysis was conducted using a Beckman Coulter System Gold Bioessential 125/168 diode array detection system (Beckman Coulter Inc., Brea, CA, USA). NMR spectroscopy was conducted on a Bruker Ultrashield™ Plus 500 NMR (Bruker Corporation, Billerica, MA, USA) with TopSpin™ software (Bruker Corporation). FT-IR spectroscopy was conducted on a Bruker Tensor 27 with a Pike MIRacle™ ATR insert for solid state analysis (Pike Technologies,

Madison, WI, USA). Data were processed with Opus software (Opus Software, Inc., San Francisco, CA, USA). Transmission electron microscopy (TEM) analysis was conducted using a JEOL (Tokyo, Japan) 1200 EX Transmission Electron Microscope. The image selected was representative, not exceptional. Thermophoresis was conducted on a NanoTemper MST Monolith™ NT.115 (NanoTemper Technologies GmbH, Munich, Germany), using the intrinsic fluorescence of (2). Raman spectroscopy was conducted on a Renishaw inVia Raman Microscope with a Renishaw 15×656, 785 nm laser (Renishaw plc, Wotton-under-Edge, UK). Data were analyzed using WiRE 3.4 software by Renishaw. Chemical compounds were used as purchased without modification.

Conjugation of p-SCN-Bn-DOTA to SWCNT-Lys-NH₂ (2) and ¹¹¹In radiolabeling

Lysine-modified, Boc-deprotected SWCNTs (2) were brought to pH 8 with metal-free sodium bicarbonate before the addition of 10 molar equivalents (compared with moles of primary amine) of 2-(4-isothiocyanatobenzyl)-1,4,7,10-tetraazacyclododecane-1,4,7,10-tetraacetic acid (p-SCN-Bn-DOTA) (Macrocyclics, Dallas, TX, USA) in a 50 mL metal-free Falcon™ Tube (Fisher Scientific Inc.). The reaction vessel was left to shake at RT for 24 hours, after which the reaction was concentrated, by speed-vacuum, to 2 mL, and run through a demetalated 10 DG Desalting Column (Bio-Rad Laboratories, Hercules, CA, USA) to remove excess p-SCN-Bn-DOTA.

The product (SWCNT-Lys-DOTA) was then labeled, as previously described,⁶ with ¹¹¹In (Nordion, Ottawa, ON, Canada), and separated from radioactive impurities, namely from free, labeled DOTA and free ¹¹¹In, with another 10 DG column, at 91% radiochemical purity, to produce (5). The process was repeated after finding metal contamination and achieved a 98.7% radiochemical purity (Figure 4).

Elimination analysis

Sixteen BALB/c mice (National Cancer Institute [NCI], Frederick, MD, USA), 8–10 weeks old, were each injected intraperitoneally (IP) with 200 nCi of SWCNT-Lys-DOTA(¹¹¹In) (5) in 200 μL phosphate-buffered saline (PBS). Cage bedding was separated from feces and collected in full at 2, 6, 12, and 24 hours, each time replacing the cage with fresh bedding. At 24 hours, the mice were sacrificed, and each bedding time point was counted (Figure 5). Two identically treated mice were autopsied at 1 and 2 weeks, to examine gross organ changes.

Murine bladder content analysis

Three BALB/c mice (NCI), 8–10 weeks old, anesthetized with ketamine to prevent urination, were each injected via the tail vein with 333 nCi SWCNT-Lys-DOTA(¹¹¹In) (5) in 200 μ L PBS. After 30 minutes, the bladders were punctured with a syringe and drained of urine for analysis. An average of 112 nCi was collected per mouse, accounting for 34% of the injected dose.

Confirmation of micturated construct

One additional mouse was injected with 5 mg of SWCNT-Lys-DOTA. Sterile urine was collected over 6 hours postinjection and compared with urine collected from the same mouse before injection, by UV-Vis spectrum analysis.

In another experiment, SWCNT-Lys-DOTA(¹¹¹In) (5) was created at 97.6% radiochemical purity and injected IP, into a BALB/c mouse, in 400 μ L of saline. Urine was collected and analyzed by HPLC for UV and emitted gamma radiation traces. Urine acquired prior to injection was mixed with unlabeled SWCNT-Lys-DOTA, for confirmation of the retention time of non-mouse-passed construct. Radiation and UV traces were aligned.

Biodistribution

Five female BALB/c mice (NCI), 10–12 weeks old, received an intravenous (IV) injection (via the retroorbital sinus) of 62.9 kBq (1.7 μ Ci) of SWCNT-Lys-DOTA(¹¹¹In) (5) in 100 μ L PBS, at 98.7% radiochemical purity. All animals were sacrificed 1 hour postinjection, and tissues (blood, heart, lung, spleen, liver, kidney, stomach, intestine, muscle, and bone) were harvested, weighed, and analyzed for ¹¹¹In activity.

Radioactivity assessment in all studies was conducted with a Capintec CRC[®]-15R Dose Calibrator and ionization chamber (Capintec, Inc., Ramsey, NJ, USA) or a Packard Cobra II Auto Gamma Counter (Packard Instrument Co., Inc., Meriden, CT, USA).

All in-vivo experiments' housing and care were in accordance with the Animal Welfare Act. The animal protocols were approved by the Institutional Animal Care and Use Committee at Memorial Sloan-Kettering Cancer Center.

Albumin binding with thermophoresis

To measure the dissociation constant between SWCNT-Lys-NH₂ and human serum albumin (HSA; Sigma-Aldrich Corp), microscale thermophoresis was employed, using the Monolith NT.115 Red/Blue instrument from NanoTemper Technologies GmbH, Munich, Germany. The SWCNT-Lys-NH₂ itself was used as the fluorescent particle,

while the HSA acted as the ligand. HSA (Sigma-Aldrich Corp) was serially diluted from 87.5 g/L (above physiological concentration) to 0.0053 g/L, while the SWCNT-Lys-NH₂ was retained at a constant concentration of 1.25 μ M. Fifteen serial dilutions of (2) were analyzed, using a 1,475 nm laser for dispersion at 120 mW and a blue light-emitting diode (LED) for excitation, with a range of 455–485 nm. The fluorescence detection ranged between 510–532 nm. The fluorescence of both tryptophan residues, which partially comprise the HSA, and SWCNT-Lys-NH₂, at relevant concentrations, were compared to discount interference from protein fluorescence on the nanotube. The resulting data were imported and curve fit using the Fnorm equation (provided by NanoTemper) (Figure 6), and known concentrations of SWCNT-Lys-NH₂ and HSA using MATLAB[®] (MathWorks, Inc., Natick, MA, USA). The fit equation was superimposed on these data using Mathematica (Wolfram Research, Champaign, IL, USA). A dissociation constant (K_d) of 6.435 μ M was obtained with a coefficient of determination (R_2) of 0.9837.

NanoTemper defines Fnorm as the normalized, steady-state fluorescence ratio of concentrations at a defined higher temperature induced by the IR laser compared with concentration at a defined colder temperature.

Fnorm should not be confused with a fluorescence versus concentration chart. In the Fnorm equation, the concentration of SWCNT and its fluorescence are constant in each capillary, while the concentration of HSA is varied from zero through the physiological range. Each capillary was scanned as an internal control for equivalent fluorescence, fluorescence reflecting equivalent concentration of SWCNT-Lys-NH₂. The [bound] and [unbound] variables are determined by the device's thermophoretic analysis. K_d is thus calculated by the fitted curve.

siRNA wrapping

The 5'-(C6-NH₂) GCAAGCUGACCCUGAA-GUUCAUtt-3' sequence was obtained from Trilink Biotechnologies (San Diego, CA, USA). The sequence was covalently modified at the 5' terminus through N-hydroxysuccinimide chemistry with a VivoTag[®] 680 XL (Perkin Elmer, Waltham, MA, USA) (excitation 665 nm; emission 688; ϵ = 210,000 M⁻¹ cm⁻¹), and purified using a 10 DG size exclusion column (Bio-Rad Laboratories). Concentrations were determined by a standard curve. Purity was evaluated by the Beckman Coulter System Gold Bioessential 125/168 diode array detection system HPLC and the SpectraMax M2 UV-Vis. The concentrations of "deBoc'd" solutions of (1) and (2) were determined by absorbance at 600 nm, as described

in Figure S3. A 0.08 μM solution of siRNA-VT680, buffered to pH 5.5 with a PBS solution (137 mM NaCl, 0.5 mM Na_2HPO_4), was titrated with incremental additions of deBoc'd (1) or (2) at 37°C, and the subsequent decrease in fluorescence was monitored by recording emission spectra after each addition. Each sequential concentration measurement was performed in triplicate. Fluorescence emission measurements were recorded at 688 nm and normalized to unwrapped oligonucleotide-dye values defined as F_0 . The emission signals were volumetrically controlled for dilution effects.

Results

The described production of the lysine-based amine handles (Figure 1B) was confirmed through a battery of spectral analyses and chemical assays (Figures S1–S9, available at [Supplementary material](#)). The quality of these spectra was closely tied to the method of purification. Since modified fullerenes, including SWCNTs and C60 buckyballs, cluster or bundle when condensed,³⁴ they are not easily resolubilized in polar solutions without sonication. Our most successful purification that utilized acid–base chemistry and dialysis is described in the Materials and methods section. Both TEM and scanning electron microscope (SEM) images (Figure S1) of this bundled, purified substance (2) confirm the anisotropic nanotube framework. The bundles formed by modified fullerenes in water allowed membrane retention of the product during dialysis. A photo of the brown, solubilized product, indicative of successful functionalization can be seen (Figure S2), as well as the visually appreciable pH solubility differential. The solubility of (1) in water was found to be 18.8 g/L at pH 7, and 7.2 g/L at pH 12. The solubility of SWCNT-Lys-NH₂ (2) was 78.6 g/L at pH 7 and 2.3 g/L at pH 12, at 22°C. The enhanced solubility of (2) at neutral pH can be explained, not only by the copious functionalization, but also, by the substitution of a more solubilizing secondary amine for the tertiary amine on (1). Combined, these effects also obviate the need for a solubilizing pegylated linker in neutral and acidic protic solvents and in polar aprotic solvents.

The SWCNT core of (2) was further supported by UV-Vis spectroscopy and HPLC analysis, establishing the absence of carbon impurities and displaying the characteristic sloping absorption profile of SWCNTs, between 280 nm and 650 nm. A concentration absorbance curve was generated for SWCNT-Lys-NH₂ (2) (Figure S3). Absorbance at 600 nm = 0.1234 (x g/L) + 0.0188. The value 600 nm was chosen as it is out of the absorbance range of most aromatics. The nearly identical to (2) UV-Vis trace of (1) is also provided (Figure S3).

The degree of modification was investigated by the Kaiser/Sarin assay, which quantifies primary amines.³⁵ These results were compared with a traditional Prato reaction (Figure 1A) run in parallel. The purified, deprotected product of the 1,3-cycloaddition using H-Lys(Boc)-OH (Figure 1B), had a higher primary amine-to-carbon ratio (0.69 mmol/gram versus 0.48 mmol/gram), meaning a denser functionalization had occurred. The functionalization ratio of the H-Lys(Boc)-OH 1,3-cycloaddition product versus the traditional Prato reaction was 1.4:1 (Figure S4), allowing for further amplified delivery.³⁶ As each adduct modifies two SWCNT wall carbons, 1.16% of (1) wall carbons were modified, and 1.64% of (2) wall carbons were modified.

The presence of two protonatable amines on (2) was further supported by forward and backward pH titration studies showing two equivalence points in the basic range at pH 9.47 and pH 8.92, in RT water. The use of amines for solubilization allowed pH-dependent purification through biphasic washing and precipitation upon basification in protic solvents (Figure 1). Significant NMR and IR peak changes and stability to reverse phase, and size exclusion chromatography confirmed adducts were covalently, not noncovalently, attached.

The structure of the expected pyrrolidine adduct was supported through the evidentiary presence of amines as well as ¹³C-NMR, H-NMR, IR, and high-resolution magic-angle spinning (HR-MAS) NMR studies (Figure S5, S6). Limited IR spectra are provided in Figure 2, with a more detailed analysis, including C60 analysis, available in Figure S5.

SWCNT length polydispersity limits the utility of techniques such as mass spectroscopy and elemental analysis. Because SWCNTs are heterogeneous and notoriously yield poorly-resolved spectra, to obtain further confirmation of the adduct, the H-Lys(Boc)-OH-based reaction was repeated on a fullerene with a defined structure. The reaction with C60 buckyballs, produced a monosubstituted species C60-Lys-NH₂ (3) (Figure 3) yielding clearer, more resolved NMR data. The mass spectrometry results (Figure S7) matched those of (3), giving a peak at 868 (m/z) equating to the monoionized product and in addition, a peak at 448 (m/z) representing the same species in which both amines on the adduct were ionized. No peaks were found representing double additions to the C60, perhaps identifying an energy barrier. Polyadducted species were beyond the range of the instrument but are considered in Figure S7A. The mass spectrum of the Boc-protected product (4) (Figure 3) produced a single peak at 479 (m/z),

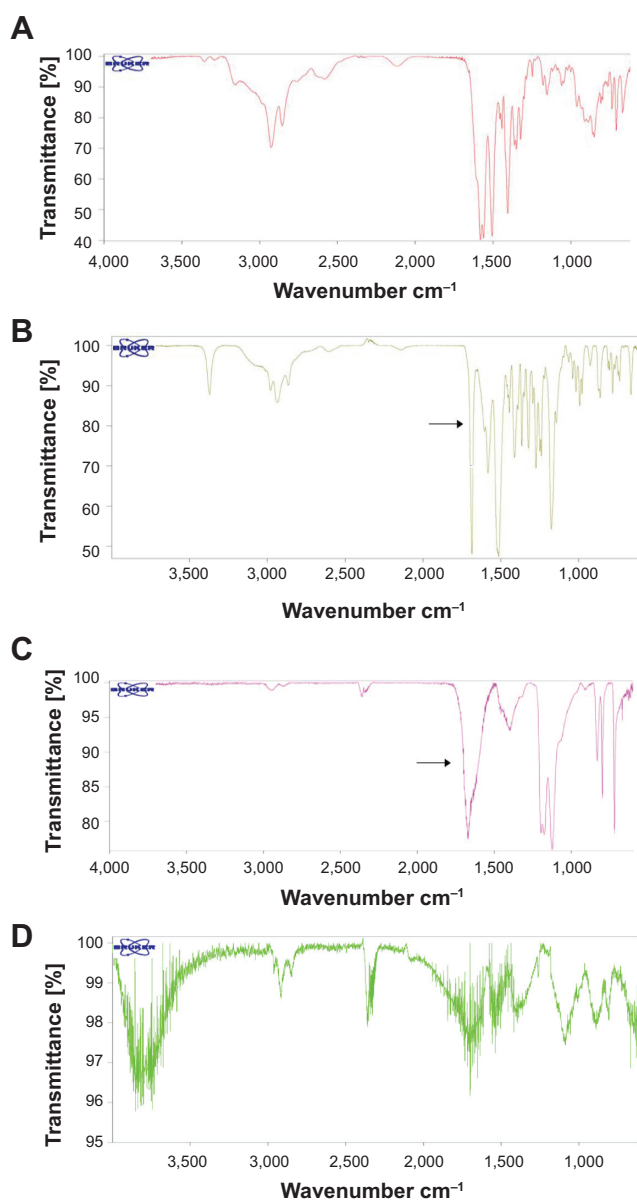


Figure 2 IR spectra of (A) L-lysine, (B) H-Lys(Boc)-OH (starting material), (C) modified SWCNT-Lys-NH₂ and (D) unpurified SWCNTs provided by Sigma-Aldrich Corporation.

Notes: The black arrow identifies the carbonyl group from the Boc moiety when present. C-H stretches found in unpurified SWCNT represent amorphous carbon impurities prior to removal. A more complete analysis is found in Figure S5.

Abbreviations: IR, infrared; SWCNT, single-walled carbon nanotube; Boc (tert-Butyloxycarbonyl); Lys, lysine.

representing a double charged cation. The relevant IR peaks found on the modified C60 mirrored those on the modified SWCNT (Figure S5).

C60 required temperatures of only 100°C compared with the 130°C required for SWCNTs. This reflects the reaction-promoting steric strain of C60. It also correlates with the difference, calculated computationally, in the binding energy of azomethine ylides with C60 and with SWCNT.³⁷

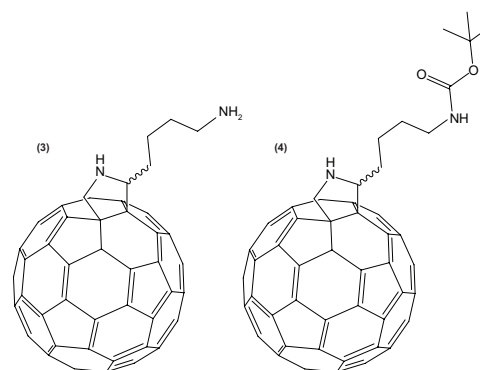


Figure 3 C60-Lys-NH₂ (3) and C60-Lys-Boc.

Abbreviations: C60, buckminsterfullerene; Boc (tert-Butyloxycarbonyl); Lys, lysine.

Evidence of the lysine adduct to C60, (3), was attained from H-NMR and ¹³C-NMR spectroscopy. Due to concerns with bundling and aggregation, the spin function when using solvent, or HR-MAS in solid state, was vital to the collection of well-defined peaks when attempting H-NMR on either C60 or SWCNTs (Figure S6).

The carbon side chain on (2) is thought to grant greater stability to the adduct than the longer ethoxy chain of (1). A comparison of the (1) and (2) starting amino acids was conducted by NMR after the samples were stored at RT in NMR tubes for approximately 1 month. H-Lys(Boc)-OH was unchanged from its initial measurements, while after 1 month, additional peaks were seen in the modified glycine of (2), suggesting partial ethoxy chain decomposition (Figure S8).

Raman spectra of (2) and its unmodified starting material are provided in Figure S9, showing expected diminution of the characteristic G band, and D band enhancement upon heavy modification.^{8,38,39}

Confirmation, through application of SWCNT functionalization, was accomplished by attaching chelating agent p-SCN-Bn-DOTA through amine-isothiocyanate bonds to the SWCNT-Lys-NH₂ amine handles. The chelator was then radiolabeled with ¹¹¹In as a tracer (Figure 4). Radioactivity and purity assessments of (5) demonstrated, not only the successful attachment of chelates, but indirectly, the substitutional reactivity of the amine handles to which the chelator was covalently bound.

These trace radiolabeled macromolecules of (5) were employed in murine elimination studies where rapid renal clearance was demonstrated. The majority of urinary excretion from an IP injection of tracer was found in the earliest (2 hour) time point, in a pharmacokinetic and biodistribution study. After 12 hours, no further radiation was found in the urine or feces. A total of 1.8% of the injected dose was recovered from

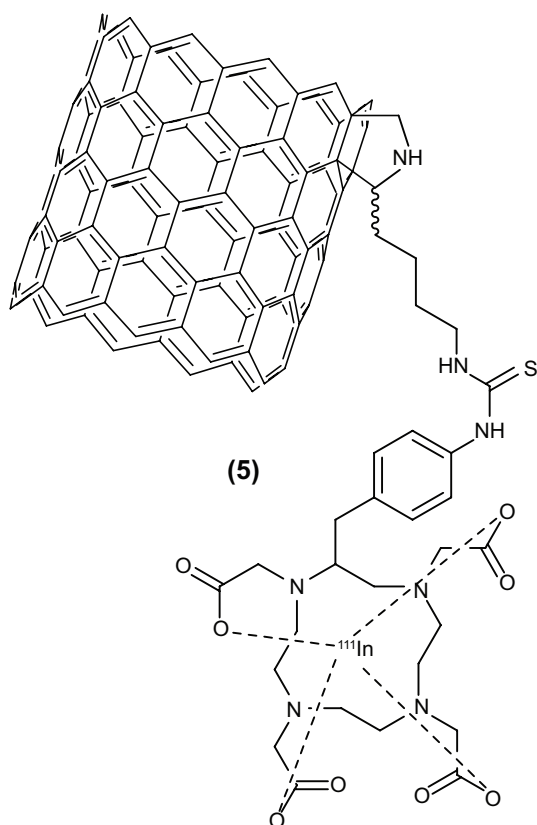


Figure 4 Structure of SWCNT-Lys-DOTA(¹¹¹In).

Abbreviations: DOTA, 1,4,7,10-tetraazacyclododecane-1,4,7,10-tetraacetic acid; SWCNT, single-walled carbon nanotube; Lys, lysine.

the feces. A total of 91.4% of the injected dose was recovered from excreted urine. The urine excretion values are regarded as a minimum because urine adhered to feces and fur was counted as feces and carcass, respectively.

The above experiment was conducted with a 98.7% high radiochemical purity labeling. Clearance studies performed with a lower radiochemical purity sample can determine whether the labeled nanotubes injected radiolabelled impurities comprise the residual corporeal activity. Injection of SWCNT-Lys-DOTA(¹¹¹In) with the lower radiochemical purity of 91.0% showed more activity remaining in the carcass (Figure 5A), providing evidence that the labeled product (5) when pure, clears more completely. The vast majority of the 6.8% of activity found in the carcass is due to deposition of the urine on the animal after micturition and the 1.3% activity unbound to the nanotube.

A urine-collection experiment of (5), via bladder puncture after an IV injection, was performed on three additional mice. An IV injection, unlike an IP injection, allows the injected compound immediate access to glomerular filtration and focuses on the actions of the kidneys. In the first 30 minutes,

an average of $34\% \pm 3.6\%$ of the injected dose was removed from the bladder by syringe.

To show that the intact SWCNT constructs were appearing in the urine, two experiments were conducted. First, 5 mg of SWCNT-Lys-DOTA were injected IP into a mouse, followed by sterile urine collection over 6 hours. The material was checked for UV-Vis absorbance and had the characteristic slope of SWCNTs after background subtraction for urine from the same mouse (taken prior to the injection of SWCNT-Lys-DOTA). Therefore, SWCNTs were entering the bladder.

Second, to ensure that the SWCNTs still had the tracer attached when excreted and that the radiolabel had not been detached by metabolism *in vivo*, the radioactive urine was collected and run on HPLC using a radiodetector. Following this, unlabeled SWCNT-Lys-DOTA in a large enough amount to be prominently seen above urine peaks was mixed with cold urine from the same mouse and run under the same conditions, employing the same HPLC UV-Vis detector. The retention times of the gamma radiation and UV peaks paired (Figure S10).

Additionally a full IV biodistribution of (5) was completed (Figure 5B), showing, in accordance with the above and prior elimination studies, that only a small percentage of the injected dose remained in the mouse after 90 minutes.^{32,40} The majority of that activity was found in the kidneys, with lesser amounts found in the liver and digestive tract. The liver, while the primary point of accumulation for unmodified SWCNTs, is a distant second in the case of functionalized tubes, with only 0.2%–0.3% of the injected dose at 12 hours postinjection. These results show better clearance and less kidney accumulation compared with results from this laboratory in a biodistribution study of radiolabeled (1).⁸

To elucidate the binding between SWCNT-Lys-NH₂ and HSA, microscale thermophoresis was employed as described in “Materials and methods” and Figure 6. At HSA concentrations up to 87.5 g/L, approximately twice physiological concentration, and a fixed SWCNT-Lys-NH₂ concentration of 1.25 μM, a single sigmoidal curve was obtained.

This sigmoidal curve plots the steady state fluorescence ratio of concentrations at a higher temperature, induced by an IR laser, compared with concentration at a colder temperature and is indicative of one bimolecular binding interaction in the measured range between the modified SWCNT and HSA. The high concentration plateau eliminates viscosity as a confounder in the solutions employed. Curve-fitting in MATLAB yielded a K_d of 6.435 μM with an R^2 of 0.9837.

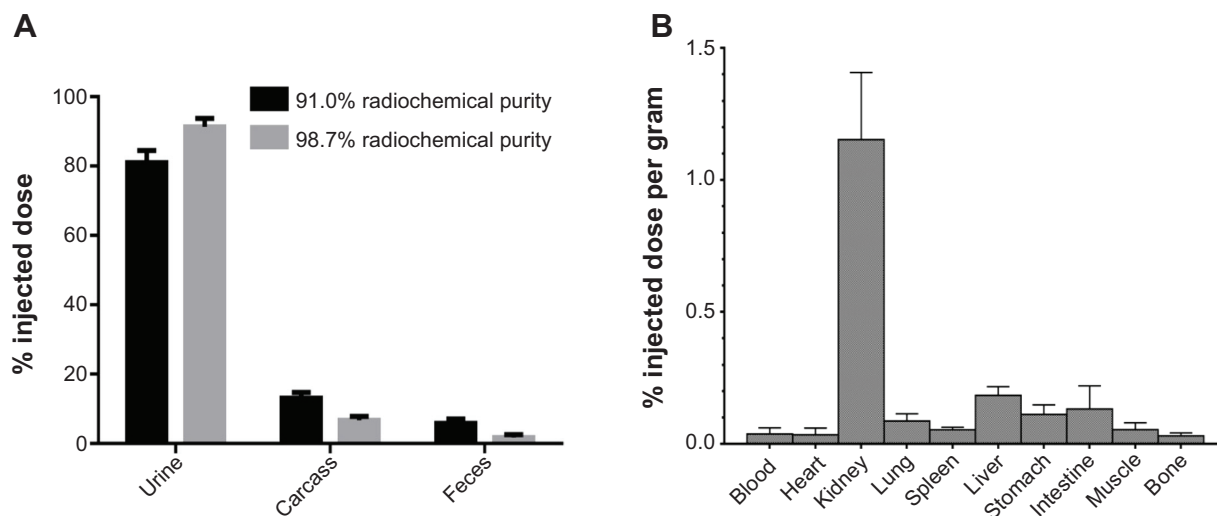


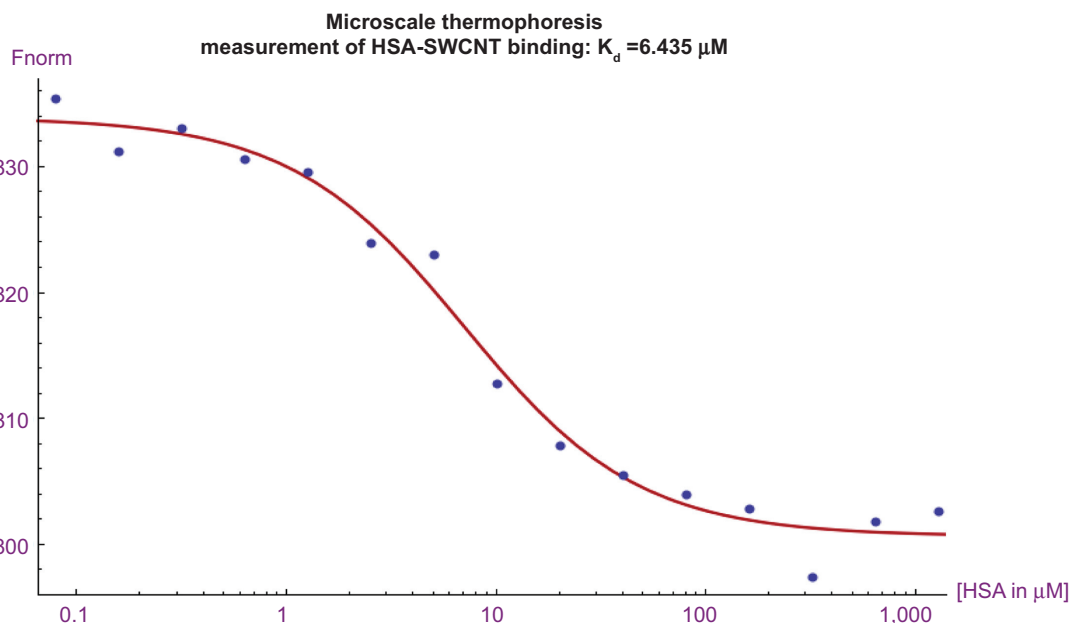
Figure 5 (A) Summed data of 16 mice in four cages with one data point per cage, 12 hours postinjection. The experiment was conducted on two different radiochemical purities of SWCNT-Lys-DOTA(¹¹¹In) (5). Total measured radiation per cage was taken as 100%, accounting for decay. **(B)** Biodistribution measuring activity of 98.7% radiochemical purity SWCNT-Lys-DOTA(¹¹¹In) (5) at 90 minutes post IV injection. N=5 mice.

Note: Error bars represent standard deviation.

Abbreviations: DOTA, 1,4,7,10-tetraazacyclododecane^{-1,4,7,10}-tetraacetic acid; IV, intravenous; SWCNT, single-walled carbon nanotube; Lys, lysine.

According to these data, a fraction of the injected construct should be bound to HSA in-vivo; because the measurements were performed at room temperature, the bound fraction may be lower at physiologic temperatures. It is significant to note that since carbon nanotubes are intrinsically fluorescent,

they act as reporters in addition to ligands in thermophoretic binding experiments. This obviates the need to functionalize the nanotubes with a fluorophore before measuring their interaction with another macromolecule. Usually thermophoresis requires a fluorophore to be conjugated to one of the materials



$$F_{norm}([HSA]) = [unbound] + \frac{1}{2}([bound] - [unbound]) \cdot \left([SWCNT] + [HSA] + K_d - \sqrt{([SWCNT] + [HSA] + K_d)^2 - 4[SWCNT][HSA]} \right)$$

Figure 6 Microscale thermophoretic K_d for first-order binding of HSA and SWCNT-Lys-NH₂.

Notes: Further statistical analysis and information on thermophoresis is found in the “Materials and methods” section. Manufacturer Nanotemper Technologies, Munich Germany.

Abbreviations: HSA, human serum albumin; SWCNT, single-walled carbon nanotube; Lys, lysine.

used in the analysis. SWCNTs are ideal because they require no deforming attachment as, even modified nanotubes, though far less fluorescent than unmodified nanotubes, produce adequate fluorescence above background to be used in thermophoretic experiments. SWCNT-Lys-NH₂ fluoresced at more than tenfold higher intensity than that of the HSA, marginalizing tryptophan fluorescence as a contributing confounder. The combination of accuracy and circumvention of this confounding variable identifies microscale thermophoresis as an especially useful technique for future fullerene binding studies in the field.

Albumin was chosen, not only because of its availability and high percentage of blood protein makeup, but also, because at blood pH, it has a high negative charge of -17 , so the modified tubes having a positive charge are more likely to have a nonspecific affinity. Because of these electrostatic forces, HSA could be considered an upper limit for the nonspecific binding of SWCNT-Lys-NH₂ to blood proteins.

Construct (2) compared favorably with (1) in the ability to wrap siRNA, using techniques previously described.⁴¹ The lack of a pegylated side did not affect small interfering (siRNA)-wrapping or was compensated by the additional density of the modification, proximity to the construct, or the amine environment (Figure 7) at pH 7.4, showing similar stoichiometry (one to two siRNA per tube) and K_d (1.108×10^{-8}) in the ten nanomolar range. Along with the previously mentioned animal studies, the successful wrapping of

siRNA on SWCNTs, a recently proposed delivery method for gene suppression,³² highlights the *in vivo* potential of modified SWCNTs.

Conclusion

Lysine has been used previously to solubilize nanotubes, through covalent attachment to multiwalled tube carboxyl groups⁴² and also noncovalently,^{43,44} but this study represents the first analysis of a covalent, side-wall adduct. While the benefits of (2) are examined herein, (1) may still be a superior choice for some applications. (1)'s ethoxy spacing moiety is twice the length, which may be important when sterically hindered additions of large molecules are desired. In addition, at basic pH, (1) exhibits a higher solubility. That said, with comparatively low-cost reagent availability, high solubility, high stability, high functionalization ratio, and new purification opportunities, the use of H-Lys(Boc)-OH in the amination of SWCNTs, by which myriad adducts may be covalently attached, should speed the translation of SWCNTs into biomedical, engineering, and *in-vivo* fields.

Acknowledgments

This work was supported by the US Department of Energy (grant number DE-SC0002456), the National Institutes of Health (grant numbers R01 CA055349, R01 CA166078, R01 CA55399, R21 CA128406, DP2-HD075698, GM07739, and P01 CA33049), the Memorial

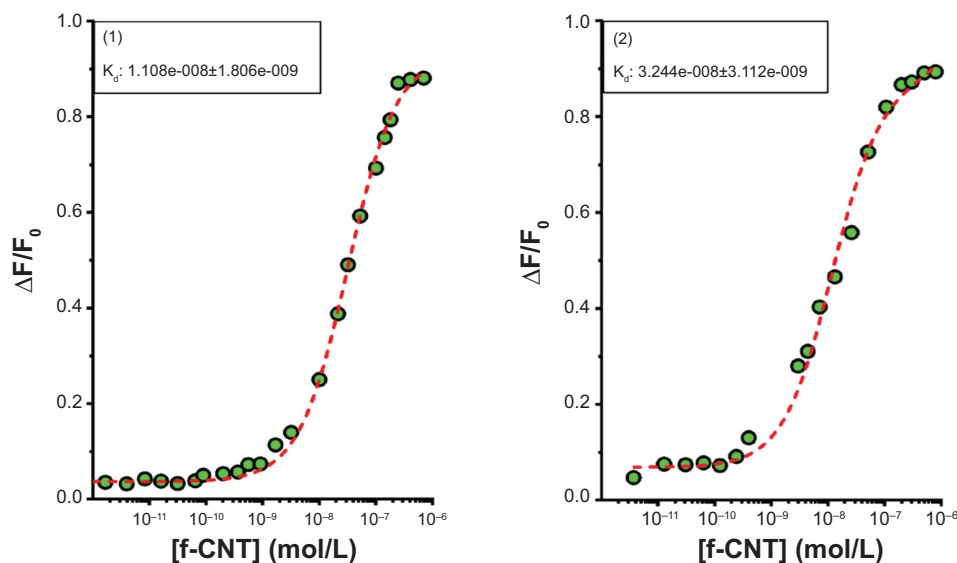


Figure 7 Comparative siRNA wrapping on (1) and (2) measured via fluorescence quenching by aromatic bases.

Notes: f-CNT refers to concentration of the functionalized carbon nanotube.

Abbreviations: F, fluorescence; siRNA, small interfering RNA; SWCNT, single wall carbon nanotube.

Sloane-Kettering Cancer Center Nano-Technology and Experimental Therapeutics Center, the National Cancer Center (grant number CA062948), The Gerstner Sloan-Kettering Undergraduate Research Program, and The Yale Mellon Research Grant.

The author thank Antonio Luz of The Rockefeller University, for thermophoresis training, and Memorial Sloan-Kettering Cancer Center personnel: Nina Lampen of the Electron Microscopy Core, Rong Wang of the Mass Spectroscopy Core, George Sukenick of the NMR Core, and Derek Tan of the Molecular Pharmacology Department.

Disclosure

The authors report no conflicts of interest in this work.

References

- Ando T. The electronic properties of graphene and carbon nanotubes. *NPG Asia Mater.* 2009;1:17–21.
- Wong EW, Sheehan PE, Lieber CM. Nanobeam mechanics: elasticity, strength, and toughness of nanorods and nanotubes. *Science.* 1997; 277(5334):1971–1975.
- Heller DA, Jin H, Martinez BM, et al. Multimodal optical sensing and analyte specificity using single-walled carbon nanotubes. *Nat Nanotechnol.* 2009;4:114–120.
- Zheng M, Jagota A, Semke ED, et al. DNA-assisted dispersion and separation of carbon nanotubes. *Nat Mater.* 2003;2:338–342.
- Wu Y, Phillips JA, Liu H, Yang R, Tan W. Carbon nanotubes protect DNA strands during cellular delivery. *ACS Nano.* 2008;2(10):2023–2028.
- Liu Z, Sun X, Nakayama-Ratchford N, Dai H. Supramolecular chemistry on water-soluble carbon nanotubes for drug loading and delivery. *ACS Nano.* 2007;1(1):50–56.
- McDevitt MR, Chattopadhyay D, Kappel BJ, et al. Tumor targeting with antibody-functionalized, radiolabeled carbon nanotubes. *J Nucl Med.* 2007;48(7):1180–1189.
- McDevitt MR, Chattopadhyay D, Jaggi JS, et al. PET imaging of soluble yttrium-86-labeled carbon nanotubes in mice. *PLoS One.* 2007;2(9):e907.
- Villa CH, McDevitt MR, Escorcía FE, et al. Synthesis and biodistribution of oligonucleotide-functionalized, tumor-targetable carbon nanotubes. *Nano Lett.* 2008;8(12):4221–4228.
- Flavin K, Lawrence K, Bartelmess J, et al. Synthesis and characterization of boron azadipyromethene single-wall carbon nanotube electron donor–acceptor conjugates. *ACS Nano.* 2011;5(2):1198–1206.
- Dhar S, Liu Z, Thomale J, Dai H, Lippard SJ. Targeted single-wall carbon nanotube-mediated Pt(IV) prodrug delivery using folate as a homing device. *J Am Chem Soc.* 2008;130(34):11467–11476.
- Shim M, Shi Kam NW, Chen RJ, Li Y, Dai H. Functionalization of carbon nanotubes for biocompatibility and biomolecular recognition. *Nano Lett.* 2002;2(4):285–288.
- Chen J, Chen S, Zhao X, Kuznetsova LV, Wong SS, Ojima I. Functionalized single-walled carbon nanotubes as rationally designed vehicles for tumor-targeted drug delivery. *J Am Chem Soc.* 2008;130(49): 16778–16785.
- Denis PA. Interaction between alkyl radicals and single wall carbon nanotubes. *J Comput Chem.* 2012;33:1511–1516.
- Liang F, Sadana AK, Peera A, et al. A convenient route to functionalized carbon nanotubes. *Nano Lett.* 2004;4(7):1257–1260.
- Bingel C. Cyclopropanierung von fullerenen. *Chem Ber.* 1993;126(8): 1957–1959.
- Camps X, Hirsch A. Efficient cyclopropanation of C 60 starting from malonates. *Journal of the Chemical Society, Perkin Transactions 1.* 1997;(11):1595–1596.
- Otohiko Tsuge, Shuji Kanemasa. Recent Advance Azomethine Ylide Chemistry Alan R. Katritzky, Editor(s), *Advances in Heterocyclic Chemistry*, Academic Press, 1989, Volume 45, Pages 231–349, ISSN 0065-2725 ISBN 9780120206452, [http://dx.doi.org/10.1016/S0065-2725\(08\)60332-3](http://dx.doi.org/10.1016/S0065-2725(08)60332-3). (<http://www.sciencedirect.com/science/article/pii/S0065272508603323>).
- Georgakilas V, Kordatos K, Prato M, Guldi DM, Holzinger M, Hirsch A. Organic functionalization of carbon nanotubes. *J Am Chem Soc.* 2002; 124:760–761.
- Bahr JL, Tour JM. Covalent chemistry of single-wall carbon nanotubes. *J Mater Chem.* 2002;12:1952–1958.
- Sawamura M, Toganoh M, Suzuki K, Hirai A, Iikura H, Nakamura E. Stepwise synthesis of fullerene cyclopentadienide R(5)C(60)(-) and indenide R(3)C(60)(-). An approach to fully unsymmetrically substituted derivatives. *Org Lett.* 2000;2(13):1919–1921.
- Methano- and Propanofullerenes by [1 + 2] and [3 + 2] Cycloadditions of Vinylcarbene Species Hidetoshi Tokuyama, Hiroyuki Isobe, Eiichi Nakamura Bulletin of the Chemical Society of Japan Vol. 68 (1995) No. 3 P 935–941.
- Matsuo Y, Iwashita A, Abe Y, et al. Regioselective synthesis of 1,4-Di(organo)[60]fullerenes through DMF-assisted monoaddition of silylmethyl grignard reagents and subsequent alkylation reaction. *J Am Chem Soc.* 2008;130(46):15429–15436.
- Hirsch A, Brettreich M. *Fullerenes: Chemistry and Reactions*. Weinheim: Wiley; 2005.
- Li Y, Lei X, Lawler RG, Murata Y, Komatsu K, Turro NJ. Synthesis and characterization of bispyrrolidine derivatives of H₂@C60: differentiation of isomers using ¹H NMR spectroscopy of endohedral H₂. *Chem Commun.* 2011;47:2282–2284.
- Schipper ML, Nakayama-Ratchford N, Davis CR, et al. A pilot toxicology study of single-walled carbon nanotubes in a small sample of mice. *Nat Nanotechnol.* 2008;3:216–221.
- Singh R, Pantarotto D, Lacerda L, et al. Tissue biodistribution and blood clearance rates of intravenously administered carbon nanotube radiotracers. *Proc Natl Acad Sci.* 2006;103(9):3357–3362.
- Dumortier H, Lacotte S, Pastorin G, et al. Functionalized carbon nanotubes are non-cytotoxic and preserve the functionality of primary immune cells. *Nano Lett.* 2006;6(7):1522–1528.
- De Volder MF, Tawfick SH, Baughman RH, Hart AJ. Carbon nanotubes: present and future commercial applications. *Science.* 2013; 339(6119): 535–539.
- Provider: John Wiley & Sons, Ltd. *Toxicity of Carbon Nanotubes: Handbook of Green Chemistry*. Weinheim: Wiley-VCH; 2012: 175–216.
- Movia D, Prina-Mello A, Bazou D, Volkov Y, Giordani S. Screening the cytotoxicity of single-walled carbon nanotubes using novel 3D tissue-mimetic models. *ACS Nano.* 2011;5(11):9278–9290.
- Mulvey JJ, Villa CH, McDevitt MR, Escorcía FE, Casey E, Scheinberg DA. Self-assembly of carbon nanotubes and antibodies on tumours for targeted amplified delivery. *Nature nanotechnology.* 2013;8(10): 763–771.
- Maggini M, Scorrano G, Prato M. Addition of azomethine ylides to C60: synthesis, characterization, and functionalization of fullerene pyrrolidines. *J Am Chem Soc.* 1993;115(21):9798–9799.
- Pantarotto D, Singh R, McCarthy D, et al. Functionalized carbon nanotubes for plasmid DNA gene delivery. *Angew Chemie Int Ed.* 2004; 43(39):5242–5246.
- Sarin VK, Kent SB, Tam JP, Merrifield RB. Quantitative monitoring of solid-phase peptide synthesis by the ninhydrin reaction. *Anal Biochem.* 1981;117(1):147–57.
- He J, Liu G, Gupta S, Zhang Y, Rusckowski M, Hnatowich DJ. Amplification targeting: a modified pretargeting approach with potential for signal amplification – proof of a concept. *J Nucl Med.* 2004;45: 1087–1095.
- Denis PA, Iribarne F. The 1,3 dipolar cycloaddition of azomethine ylides to graphene, single wall carbon nanotubes, and C60. *Int J Quantum Chem.* 2010;110(9):1764–1771.

38. Hussain S, et al. "Spectroscopic investigation of modified single wall carbon nanotube (SWCNT)." *Journal of Modern Physics*. 2011;2.06:538.
39. Lin Y, Zhou B, Martin RB, et al. Visible luminescence of carbon nanotubes and dependence on functionalization. *J Phys Chem B*. 2005; 109(31):14779–14782.
40. Ruggiero A, Villa CH, Bander E, et al. Paradoxical glomerular filtration of carbon nanotubes. *Proc Natl Acad Sci*. 2010;107(27):12369–12374.
41. Deploying RNA and DNA with Functionalized Carbon Nanotubes. *J Phys Chem C Nanomater Interfaces*. 2013;117(11):5982–5992.
42. Hu N, Dang G, Zhou H, Jing J, Chen C. Efficient direct water dispersion of multi-walled carbon nanotubes by functionalization with lysine. *Mater Lett*. 2007;61(30):5285–5287.
43. Piao L, Liu Q, Li Y. Interaction of amino acids and single-wall carbon nanotubes. *J Phys Chem*. 2012;116(2):1724–1731.
44. Kim JB, Premkumar T, Giani O, Robin JJ, Schue F, Geckeler KE. Nanocomposites of poly(L-lysine) and single-walled carbon nanotubes. *Polym Internat*. 2008;57:311–315.

International Journal of Nanomedicine

Publish your work in this journal

The International Journal of Nanomedicine is an international, peer-reviewed journal focusing on the application of nanotechnology in diagnostics, therapeutics, and drug delivery systems throughout the biomedical field. This journal is indexed on PubMed Central, MedLine, CAS, SciSearch®, Current Contents®/Clinical Medicine,

Submit your manuscript here: <http://www.dovepress.com/international-journal-of-nanomedicine-journal>

Journal Citation Reports/Science Edition, EMBase, Scopus and the Elsevier Bibliographic databases. The manuscript management system is completely online and includes a very quick and fair peer-review system, which is all easy to use. Visit <http://www.dovepress.com/testimonials.php> to read real quotes from published authors.

Dovepress